

Correlation function of the luminosity distances

Sang Gyu Biern^{a,c} and Jaiyul Yoo^{a,b}

^aCenter for Theoretical Astrophysics and Cosmology, Institute for Computational Science, University of Zürich, Winterthurerstrasse 190, CH-8057, Zürich, Switzerland

^bPhysics Institute, University of Zürich, Winterthurerstrasse 190, CH-8057, Zürich, Switzerland

^cAsia Pacific Center for Theoretical Physics, Pohang, 790-784, Korea

E-mail: sgbiern@physik.uzh.ch, jyoo@physik.uzh.ch

Abstract. We present the correlation function of the luminosity distances in a flat Λ CDM universe. Decomposing the luminosity distance fluctuation into the velocity, the gravitational potential, and the lensing contributions in linear perturbation theory, we study their individual contributions to the correlation function. The lensing contribution is important at large redshift ($z \gtrsim 0.5$) but only for small angular separation ($\theta \lesssim 3^\circ$), while the velocity contribution dominates over the other contributions at low redshift or at larger separation. However, the gravitational potential contribution is always subdominant at all scale, if the correct gauge-invariant expression is used. The correlation function of the luminosity distances depends significantly on the matter content, especially for the lensing contribution, thus providing a novel tool of estimating cosmological parameters.

Contents

1	Introduction	1
2	Luminosity distance in an inhomogeneous universe	3
3	Analytic expressions for the two-point correlation function of the luminosity distances	4
4	Results	7
4.1	Angular correlation function of the luminosity distance ($z_1 = z_2$)	7
4.2	Three-dimensional two-point correlation function of the luminosity distance ($z_1 \neq z_2$)	8
5	Discussion	12
A	The auto-correlation function of the gravitational potential contribution	14

1 Introduction

One of great mysteries of current physics is the accelerating expansion of the universe. This acceleration was first revealed by measuring the luminosity distances of distant supernovae [1, 2], and following measurements of the microwave background anisotropies (e.g. [3]) and the acoustic peak position in galaxy clustering (e.g. [4]) have supported this phenomenon. However, despite the fact that the universe is inhomogeneous and anisotropic, the effects of inhomogeneity have been commonly dismissed in interpreting the luminosity distance measurements.

There are several theoretical efforts of deriving the luminosity distance fluctuation, accounting for the inhomogeneities in our Universe [6, 10, 18, 20, 21]. The fluctuation in the luminosity distance was first derived by Sasaki [6] from the Sachs approach. Later studies computed the fluctuation in the luminosity distance by utilizing the Jacobi mapping [10], the Geodesic-Light-Cone gauge approach [12–17], and the geometric approach [7, 8].

Using the full expression of the luminosity distance, the angular power spectrum was derived in [10]. The detectability of the power spectrum and the correlation function of the gravitational lensing contribution was investigated in [23, 24]. These studies show that the lensing power spectrum/correlation can be measured in a high- z and a deep survey such as the Large Synoptic Sky Telescope survey (LSST) [5], and by using the supernova lensing dispersion, [34–36] present the way of constraining the properties of the primordial power spectrum. In addition to the lensing contribution, there exist other contributions to the luminosity distance, such as the velocity and the gravitational potential, and these contributions are all correlated. Thus, a proper computation of its correlation function should account for all these additional components. In particular, the gravitational potential contribution to the luminosity distance correlation has not been *properly* considered in literature.

Furthermore, the correlated fluctuations in the luminosity distance can significantly affect the covariance matrix of the (apparent-) magnitude of supernovae, used for the cosmological parameter estimation in supernova surveys. In [21], it was shown that the systematic errors from the velocity contribution, induced by the large scale structure of the universe, can substantially bias the covariance matrix of the magnitude of supernovae. This study shows that there is a significant degradation in the determination of the dark energy equation of state.

Within the framework of cosmological perturbation theory, the observed luminosity distance fluctuation at the linear order consists of the velocity at the positions of observation and source, the lensing,

and the gravitational potential contributions, but either the velocity at the observer position and/or the gravitational potential contributions are not considered in the previous luminosity distance correlation related studies (e.g., [15, 33]). First, although the expressions of all the contributions are presented in literature, the gravitational potential contribution is always neglected in numerical computations related to the luminosity distance correlation function, arguing that it is suppressed compared to the other contributions. Second, the contribution of the velocity at the observation is turned off by hand because the observer’s peculiar motion is corrected in the luminosity distance measurement by using the dipole of the cosmic microwave background radiation (CMB) observation.

In [18], it was demonstrated that the commonly used expression for the luminosity distance often lacks the coordinate lapse $\delta\tau_o$ at the observer position and its variance is infrared divergent. This infrared divergence in the luminosity distance variance originates from the gravitational potential contribution, and hence one naturally expects that the gravitational potential contribution can be the most dominant contribution in the expression of the previous studies. Despite the presence of such infrared divergences, this pathology in the luminosity distance has been commonly dismissed by considering only the sub-horizon perturbation mode (i.e., by introducing an *ad hoc* cutoff k_{IR} as $k_{\text{IR}} \simeq \mathcal{H}_o$, where \mathcal{H}_o is the current Hubble parameter). In fact, as shown in [18], the luminosity distance is devoid of the infrared divergence when one considers the missing coordinate lapse and all the other contributions of the gravitational potential to the luminosity distance. Here we compute the gravitational potential contribution to the correlation function, and we show that it always contributes little to the correlation function of the luminosity distances.

Furthermore, we also consider the velocity contribution at the observation position for two physical reasons: gauge invariance and equivalence principle. Without the velocity contribution at the observer position, the gauge-invariance of the expression for the luminosity distance is broken, and the uniform gravity-mode affects the resulting outcome, in direct conflict with the equivalence principle, as shown in [8, 18]. Practically, as opposed to the gravitational potential contribution, the velocity contribution at the observation is substantial, especially at small redshift. Thus, neglecting the velocity contribution at the observation causes not only the theoretical problems but also significant numerical errors. Therefore, we consider all the contributions to the luminosity distance correlation function. We further investigate how the correlation function varies with respect to the matter content.

Before we proceed, we stress the critical difference in various terms referring to the peculiar velocity at the observer position. Within the framework of cosmological perturbation theory, the peculiar velocity field is well defined, and the peculiar velocity at the observer position is naturally called the peculiar velocity of the observer. However, these perturbations are gauge-dependent; their values change depending on our choice of coordinate systems. For example, the peculiar velocity field in the synchronous gauge is zero everywhere at the linear order in perturbations, while it is non-vanishing in the conformal Newtonian gauge. Therefore, these peculiar velocities at the observer position also depend on gauge choice, and these perturbations themselves cannot have any physical meaning.

However, there exists a physically well-defined peculiar velocity of the observer often used in literature, with which we can transform to a frame where the CMB dipole vanishes. This peculiar velocity ($v_{\text{dip}} \simeq 371 \text{ km/s}$ [25]) is independent of our gauge choice, and it is *not* identical to the peculiar velocity at the observer position in either the conformal Newtonian gauge or the synchronous gauge. It will be referred to as the peculiar velocity of the observer with respect to the CMB rest frame, or the observed peculiar velocity. We will discuss its impact on the luminosity distance measurements in Sec. 5. Unless mentioned explicitly, the peculiar velocity in this paper means the peculiar velocity in cosmological perturbation theory.

This paper is organized as follows: In section 2, we review the linear-order luminosity distance fluctuation and decompose it into the velocity, the gravitational potential, and the lensing contributions.

In section 3, we present the analytic expressions of the correlation functions of the velocity, the lensing, and the (simplified) gravitational potential contributions. The numerical results are shown in section 4: the angular correlation function in section 4.1, and the three-dimensional two-point correlation function in section 4.2. Especially, in section 4.1, we investigate the angular correlation function of the luminosity distances with different cosmological parameter sets. In section 5, we summarize and discuss our new results. In appendix A, we present the explicit expression of the auto-correlation function of the gravitational potential contribution.

2 Luminosity distance in an inhomogeneous universe

In this section we briefly summarize the linear-order calculations of the luminosity distance. The fluctuation $\delta\mathcal{D}_L$ in the luminosity distance \mathcal{D}_L is given by [7]:

$$\mathcal{D}_L \equiv \bar{\mathcal{D}}_L(z) (1 + \delta\mathcal{D}_L), \quad \delta\mathcal{D}_L = \delta z + \frac{\delta r}{\bar{r}_z} + \Xi - \kappa, \quad (2.1)$$

where $\bar{\mathcal{D}}_L(z)$ is the luminosity distance in a homogeneous universe, δz is the redshift distortion, δr is the radial distortion, Ξ is the frame distortion, and κ is the angular distortion.

Thanks to the gauge-invariant calculation of the luminosity distance in [6], we can obtain a consistent result in any gauge choice. From now on, we shall study the luminosity distance fluctuation in the conformal Newtonian gauge. In this gauge, we decompose the luminosity distance fluctuation into the velocity $\delta\mathcal{D}_L^V$, the lensing $\delta\mathcal{D}_L^{\text{lens.}}$, and the gravitational potential $\delta\mathcal{D}_L^\Psi$ contributions i.e., $\delta\mathcal{D}_L = \delta\mathcal{D}_L^V + \delta\mathcal{D}_L^{\text{lens.}} + \delta\mathcal{D}_L^\Psi$.¹ The velocity (lensing) contribution contains single (double) spatial derivative of the gravitational potential Ψ i.e., $V_{\parallel} \propto \partial_{\parallel}\Psi$ ($\Delta\Psi$), whereas the gravitational potential contribution is free from $\partial_i^n\Psi$ for any n . These contributions to the luminosity distance are explicitly

$$\begin{aligned} \delta\mathcal{D}_L^V &= \left(1 - \frac{1}{\mathcal{H}_z \bar{r}_z}\right) V_{\parallel s} + \frac{1}{\mathcal{H}_z \bar{r}_z} V_{\parallel o}, \\ \delta\mathcal{D}_L^{\text{lens.}} &= - \int_0^{\bar{r}_z} d\bar{r} \left\{ (\bar{r}_z - \bar{r}) \frac{\bar{r}}{\bar{r}_z} \Delta\Psi \right\} = - \frac{3}{2} \mathcal{H}_o^2 \Omega_m \int_0^{\bar{r}_z} d\bar{r} \left\{ (\bar{r}_z - \bar{r}) \frac{\bar{r}}{\bar{r}_z} \frac{1}{a(\bar{\tau}_o - \bar{r})} \delta(\bar{\tau}_o - \bar{r}, \bar{r}\hat{n}) \right\}, \\ \delta\mathcal{D}_L^\Psi &= \left(\mathcal{H}_o + \frac{1}{\bar{r}_z} - \frac{\mathcal{H}_o}{\mathcal{H}_z \bar{r}_z} \right) \delta\tau_o + \frac{1}{\mathcal{H}_z \bar{r}_z} \Psi_s - \frac{1}{\mathcal{H}_z \bar{r}_z} \Psi_o - \Psi_s \\ &\quad + \int_0^{\bar{r}_z} d\bar{r} \left\{ \frac{2}{\bar{r}_z} \Psi + 2 \left(\frac{1}{\mathcal{H}_z \bar{r}_z} + \frac{\bar{r}}{\bar{r}_z} - 1 \right) \Psi' + (\bar{r}_z - \bar{r}) \frac{\bar{r}}{\bar{r}_z} \Psi'' \right\}, \end{aligned} \quad (2.2)$$

where the suffix o and s indicate that a variable is evaluated at the observation and the source, respectively. Note that we used the Poisson equation $\Delta\Psi = \frac{3}{2} \mathcal{H}_o^2 \Omega_m \delta/a$ in $\delta\mathcal{D}_L^{\text{lens.}}$, where δ is the linear-order matter density contrast in the Newtonian cosmology or the synchronous gauge. One can decompose the velocity and the potential into time-dependent and scale-dependent parts as $V_{\parallel}(\tau, \mathbf{x}) = D_V(\tau) \partial_{\parallel}\zeta(\mathbf{x})$, $\Psi(\tau, \mathbf{x}) = D_\Psi(\tau) \zeta(\mathbf{x})$, where ζ is the time-independent but scale dependent curvature perturbation. The solutions of D_V and D_Ψ in Eq. (2.2) are presented in [18, 19]. The detailed derivations of these equations are presented in [6, 7, 9].

¹In our previous paper [18], we express the gravitational potential contribution without the coordinate lapse $\delta\tau_o$ at the observation. However, in this paper we define the gravitational potential contribution by including the contribution of $\delta\tau_o$. The term $\delta\mathcal{D}_L^{\Psi+\delta\tau_o}$ in [18] corresponds to the gravitational potential contribution in this paper.

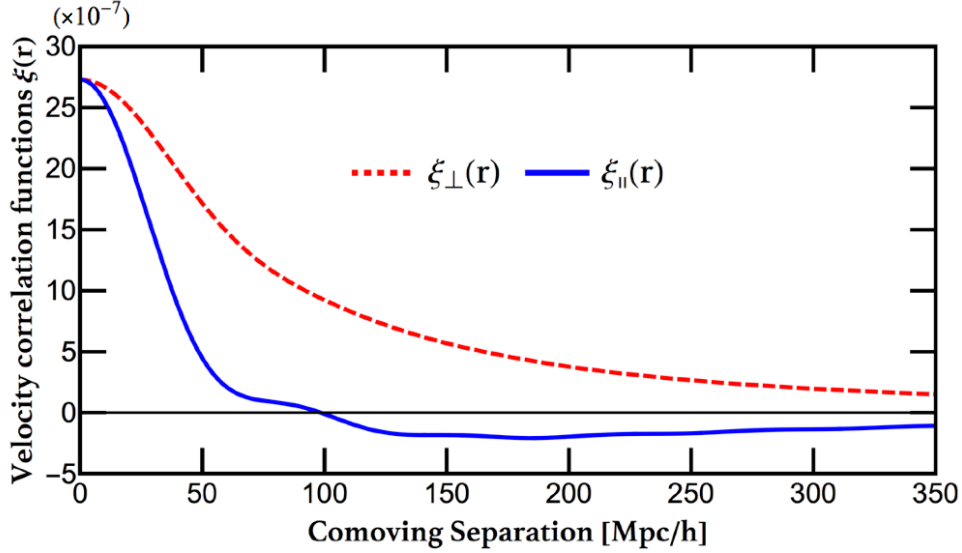


Figure 1: The velocity correlation function $\langle V_{\parallel}(z_1, \hat{n}_1)V_{\parallel}(z_2, \hat{n}_2) \rangle$ is decomposed as the correlations ξ_{\parallel} and ξ_{\perp} parallel and perpendicular to the separation vector, respectively (see Eq. (3.2)). The computations are performed under the choices of $k_{\text{IR}} = \mathcal{H}_o$ and $k_{\text{UV}} = 0.1 h/\text{Mpc}$.

3 Analytic expressions for the two-point correlation function of the luminosity distances

To derive the velocity contribution to the correlation function of the luminosity distances, we need the two-point correlation function of radial velocities: $\langle V_{\parallel}(z_1, \hat{n}_1)V_{\parallel}(z_2, \hat{n}_2) \rangle$. Using $V_{\parallel}(\tau, \mathbf{x}) = D_V(\tau)\partial_{\parallel}\zeta(\mathbf{x})$, the correlation function of the radial velocities can be expressed as

$$\langle V_{\parallel}(z_1, \hat{n}_1)V_{\parallel}(z_2, \hat{n}_2) \rangle = \hat{n}_1^i \hat{n}_2^j \langle V_i(z_1, \hat{n}_1)V_j(z_2, \hat{n}_2) \rangle = \left(\frac{\mathcal{C}}{\mathcal{H}_o} \right)^2 D_{V_1} D_{V_2} \left\{ \hat{\mathcal{P}}_{\parallel} \xi_{\parallel}(|\mathbf{r}|) + \hat{\mathcal{P}}_{\perp} \xi_{\perp}(|\mathbf{r}|) \right\}, \quad (3.1)$$

where the suffix i indicates that a temporal function is evaluated at z_i e.g., $D_{V_1} = D_V(z_1)$, and $\mathcal{C} \equiv -\frac{5}{2}\mathcal{H}_o^2\Omega_m$. Note that we decompose the velocity correlation function $\langle V_i V_j \rangle$ into the parallel and the perpendicular components with respect to the separation vector $\mathbf{r} = \bar{r}_{z_1}\hat{\mathbf{n}}_1 - \bar{r}_{z_2}\hat{\mathbf{n}}_2$: $\langle V_i V_j \rangle = \hat{r}_i \hat{r}_j \xi_{\parallel} + (\delta_{ij} - \hat{r}_i \hat{r}_j) \xi_{\perp}$, and we defined $\hat{\mathcal{P}}_{\parallel} \equiv \hat{n}_1^i \hat{n}_2^j \hat{r}_i \hat{r}_j$, and $\hat{\mathcal{P}}_{\perp} \equiv \hat{n}_1^i \hat{n}_2^j (\delta_{ij} - \hat{r}_i \hat{r}_j)$. The correlation functions of the perpendicular and the parallel components ξ_{\perp} and ξ_{\parallel} are defined respectively as

$$\xi_{\perp}(r) \equiv -\mathcal{H}_o^2 \int_{k_{\text{IR}}}^{k_{\text{UV}}} \frac{dk}{2\pi^2} P_m(k) \frac{j_0'(kr)}{kr}, \quad \xi_{\parallel}(r) \equiv -\mathcal{H}_o^2 \int_{k_{\text{IR}}}^{k_{\text{UV}}} \frac{dk}{2\pi^2} P_m(k) j_0''(kr), \quad (3.2)$$

where $j_0(x)$ is the spherical Bessel function, and $P_m(k)$ is the matter power spectrum in the synchronous gauge computed by using CAMB. k_{IR} and k_{UV} represent the lower and the upper cutoffs in the integration, respectively. Figure 1 shows ξ_{\perp} and ξ_{\parallel} with respect to the separation r . Note that $\hat{\mathcal{P}}_{\perp}$ vanishes when the line-of-sights of two sources are aligned, and the contribution of $\hat{\mathcal{P}}_{\perp}$ is the characteristic of the case $\hat{\mathbf{n}}_1 \neq \hat{\mathbf{n}}_2$ i.e., the wide angle effect.

Utilizing Eq. (3.1), one can derive the auto-correlation function of the velocity contribution:

$$\begin{aligned}
\langle \delta \mathcal{D}_L^V(z_1, \hat{\mathbf{n}}_1) \delta \mathcal{D}_L^V(z_2, \hat{\mathbf{n}}_2) \rangle &= \left(\frac{\mathcal{C}}{\mathcal{H}_o} \right)^2 D_{V_1} D_{V_2} \left(1 - \frac{1}{\mathcal{H}_{z_1} \bar{r}_{z_1}} \right) \left(1 - \frac{1}{\mathcal{H}_{z_2} \bar{r}_{z_2}} \right) \left[\hat{\mathcal{P}}_{\perp} \xi_{\perp}(|\mathbf{r}|) + \hat{\mathcal{P}}_{\parallel} \xi_{\parallel}(|\mathbf{r}|) \right] \\
&+ \left(\frac{\mathcal{C}}{\mathcal{H}_o} \right)^2 D_{V_1} D_{V_o} \frac{1}{\mathcal{H}_{z_2} \bar{r}_{z_2}} \left(1 - \frac{1}{\mathcal{H}_{z_1} \bar{r}_{z_1}} \right) \hat{\mathcal{P}}_{\parallel} \xi_{\parallel}(\bar{r}_{z_1}) + (1 \leftrightarrow 2) \\
&+ \mathcal{C}^2 D_{V_o}^2 \frac{1}{(\mathcal{H}_{z_1} \bar{r}_{z_1})} \frac{1}{(\mathcal{H}_{z_2} \bar{r}_{z_2})} \hat{\mathbf{n}}_1 \cdot \hat{\mathbf{n}}_2 \int_{k_{\text{IR}}}^{k_{\text{UV}}} \frac{dk}{6\pi^2} P_m(k). \tag{3.3}
\end{aligned}$$

As shown in Fig. 1, the velocity correlation ξ_{\perp} perpendicular to the separation is always positive, and it decays monotonically as the separation increases. The velocity correlation ξ_{\parallel} parallel to the separation also decreases monotonically as the separation increases before reaching to the sign flip ($r \simeq 100 \text{ Mpc}/h$) from positive to negative, and it is nearly independent of the separation beyond the sign flip. Note that ξ_{\parallel} and ξ_{\perp} are derived from the cutoff choices $k_{\text{IR}} = \mathcal{H}_o$ and $k_{\text{UV}} = 0.1 \text{ h}/\text{Mpc}$. The super-horizon modes contribution to ξ_{\parallel} and ξ_{\perp} is negligible, and we choose $k_{\text{IR}} = \mathcal{H}_o$. In contrast, for larger choice of k_{UV} e.g., $k_{\text{UV}} = 1 \text{ h}/\text{Mpc}$, the wiggle of ξ_{\parallel} in Fig. 1 disappears, and ξ_{\parallel} becomes a smooth function, while the shape of ξ_{\perp} does not change since the integrand of ξ_{\perp} in Eq. (3.2) is insensitive on large k . In addition to the shape-changing, in the case of the cutoff choice, the maximum values of ξ_{\parallel} and ξ_{\perp} are a factor of 1.5 larger than those in Fig. 1. However, the larger choice $k_{\text{UV}} > 1 \text{ h}/\text{Mpc}$ does not yield substantial numerical difference to ξ_{\parallel} and ξ_{\perp} .

The first line in Eq. (3.3) is the auto-correlation of the source velocity contribution. Because of the property of ξ_{\parallel} that becomes negative for large separations, the source velocity contribution to the correlation function of the luminosity distances can be anti-correlated (the directions of each velocity are opposite) when the separation is large enough and $\hat{\mathcal{P}}_{\perp} \simeq 0$. However, in other cases, the sign of this correlation function is positive.

The second line corresponds to the cross-correlation of the contributions of the velocities at source and observer positions. It vanishes when two sources are far away from the observer but with small angular separation i.e., $\hat{\mathcal{P}}_{\parallel} \simeq 0$. ($\hat{\mathbf{n}}_1 // \hat{\mathbf{n}}_2 \perp \hat{\mathbf{r}}$). However, since the comoving separation is large $\bar{r}_{z_1}, \bar{r}_{z_2} > 300 \text{ Mpc}/h$ for $z_1, z_2 > 0.1$, there is in practice a strong suppression in the integrand due to the suppression the spherical Bessel function $j_0(k\bar{r}_z)$, regardless of $\hat{\mathcal{P}}_{\parallel}$. Thus, the magnitude of the cross-correlation is much smaller than the correlation functions of the other velocity contributions.

The last line represents the auto-correlation of the contribution of the velocity at observer position, and it depends on the angular separation between sources and the source distances from the observer. Since this line is proportional to the correlation of the observer velocity components along two light-of-sights of sources, it vanishes when the angular separation between sources is 90° i.e., $\hat{\mathbf{n}}_1 \cdot \hat{\mathbf{n}}_2 = 0$ and increases as the angular separation decreases. In addition, it has a small value when the sources are far away from the observer. Apparent in Eq. (2.2), the observed luminosity distance depends on the velocity contribution at the observer position, and its ensemble average is used for computing the correlation in Eq. (3.3). The ergodic theorem says our observational average is equivalent to the average over many realizations of the Universe, and Eq. (3.3) represents we make observations over many realizations of the Universe, in which the velocity at the observer position changes.

The other important contribution is the gravitational lensing contribution. The lensing correlation function is given by

$$\langle \delta \mathcal{D}_L^{\text{lens.}}(z_1, \hat{\mathbf{n}}_1) \delta \mathcal{D}_L^{\text{lens.}}(z_2, \hat{\mathbf{n}}_2) \rangle = \frac{9}{4} \mathcal{H}_o^4 \Omega_m^2 \int_0^{\bar{r}_{z_1}} d\bar{r}_1 g(\bar{r}_1) \int_0^{\bar{r}_{z_2}} d\bar{r}_2 g(\bar{r}_2) \xi_m \left(|\bar{r}_1 \hat{\mathbf{n}}_1 - \bar{r}_2 \hat{\mathbf{n}}_2| \right), \tag{3.4}$$

where $g(\bar{r}_i) \equiv \frac{(\bar{r}_{z_i} - \bar{r}_i)\bar{r}_i}{\bar{r}_{z_i}} \frac{D(\bar{r}_o - \bar{r}_i)}{a(\bar{r}_o - \bar{r}_i)}$, and $\xi_m(|\mathbf{r}|)$ is the matter correlation function i.e., $\xi_m(|\mathbf{r}|) = \langle \delta(\mathbf{x})\delta(\mathbf{x} + \mathbf{r}) \rangle$, which decays as the separation $|\mathbf{r}|$ increases. Since we shall consider large angular separation cases, we will compute this contribution accurately instead of applying the Limber approximation, which works well only for small angular separation (e.g., see [28]).

Our numerical integration of the lensing correlation is performed along the paths of two photons emitted from two sources, and it normally increases as the distance between the observer and the source increases. However, for a large angular separation, the gravitational lensing contribution becomes quickly negligible. The reason is that the separation of the matter correlation function increases quickly with respect to \bar{r}_1 and \bar{r}_2 when the angular separation is large. That is, the matter correlation function in the integration decays sharply as \bar{r}_1 and \bar{r}_2 increase when the angular separation is large. Thus, the lensing correlation can be mostly significant for small angular separation and large redshift.

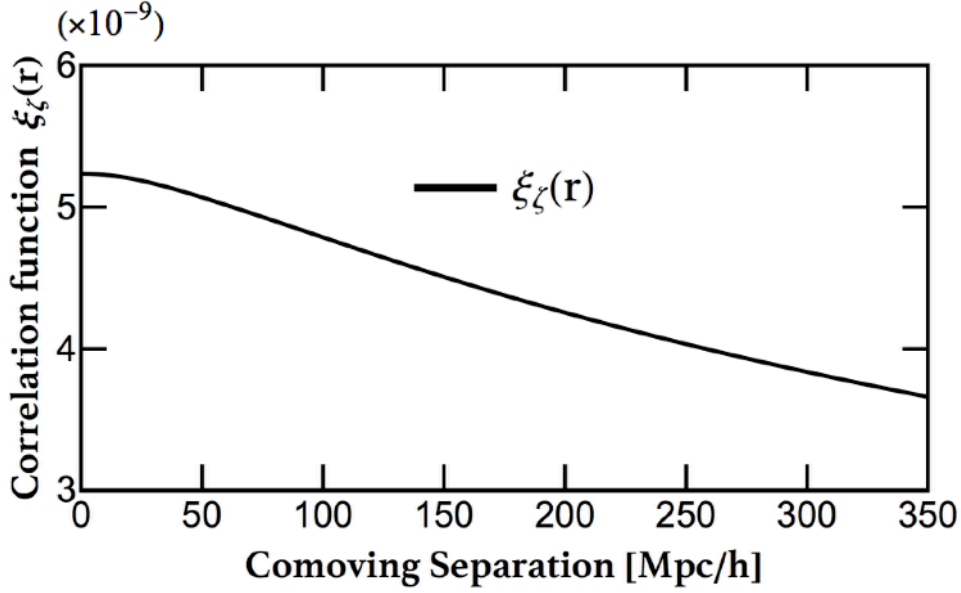


Figure 2: The auto- correlation function $\xi_\zeta(r)$ of the curvature perturbation in the Λ CDM universe ($\Omega_m = 0.3$) for $k_{\text{IR}} = \mathcal{H}_o$ and $k_{\text{UV}} = 0.1 \text{ Mpc}/h$ (see appendix A for details).

Finally, we discuss the gravitational potential contribution to the luminosity distance correlation.² The auto-correlation function of the gravitational potential is $\langle \Psi(z_1, \hat{n}_1)\Psi(z_2, \hat{n}_2) \rangle = D_\Psi(z_1)D_\Psi(z_2)\xi_\zeta(|\mathbf{r}|)$, and the correlation function ξ_ζ of the curvature perturbation in Fig. 2 is

$$\xi_\zeta(|\mathbf{r}|) \equiv \langle \zeta(\mathbf{x})\zeta(\mathbf{x} + \mathbf{r}) \rangle = \frac{25}{4} \mathcal{H}_o^4 \Omega_m^2 \int_{k_{\text{IR}}}^{k_{\text{UV}}} \frac{dk}{2\pi^2} \frac{1}{k^2} P_m(k) j_0(kr). \quad (3.5)$$

Given the red tilt of the spectral index, the correlation function (and its variance) ξ_ζ diverges as we include modes on larger scales ($k < k_{\text{IR}}$). However, as shown in [18], the contributions of the gravitational potential at $k < k_{\text{IR}}$ cancel in $\delta\mathcal{D}_L$, and their exact value is rather insensitive as long as $k_{\text{IR}} < \mathcal{H}_o$. Figure 2 and our numerical calculations of the gravitational potential represent their effective contributions to $\delta\mathcal{D}_L$ with the long-mode cancellation taken into account.

As depicted in Fig. 2, the auto-correlation function of the curvature perturbation decreases as the separation increases, but the amplitude does not change significantly. Thus, the auto-correlation

²Since the expression of the auto-correlation of the gravitational potential contribution is complicated, we present the explicit expression in appendix A.

function of the gravitational potential contribution is nearly independent of separation, and its amplitude is similar to the amplitude of the luminosity distance variance of this contribution. Since D_Ψ is nearly time-independent in a Λ CDM universe, by assuming $D_\Psi(z) = D_{\Psi_o}$ we can simplify the gravitational potential contribution for sufficiently large redshift as $\delta\mathcal{D}_L^\Psi \simeq \left(1 - \frac{1}{\mathcal{H}_z \bar{r}_z}\right) \mathcal{H}_o \delta\tau_o + 2\Psi_o = \left(1 - \frac{1}{\mathcal{H}_z \bar{r}_z}\right) (\Psi_o + \zeta_o) + 2\Psi_o$. From this, we can derive the auto-correlation function of the simplified one:

$$\langle \delta\mathcal{D}_L^\Psi(z_1, \hat{n}_1) \delta\mathcal{D}_L^\Psi(z_2, \hat{n}_2) \rangle \simeq \left\{ \left(2D_{\Psi_o} + 1 - \frac{1}{\mathcal{H}_{z_1} \bar{r}_{z_1}} (D_{\Psi_o} + 1) \right) \times (1 \leftrightarrow 2) \right\} \xi_\zeta(0). \quad (3.6)$$

The numerical value of the redshift dependent part in Eq. (3.6) is 3.7 (0.03) at $z_1 = z_2 = 0.5$ ($z_1 = z_2 = 1.0$). That is, the amplitude of the auto-correlation function of the gravitational potential contribution is approximately $\mathcal{O}(10^{-8})$ ($\mathcal{O}(10^{-10})$) at $z_1 = z_2 = 0.5$ ($z_1 = z_2 = 1.0$). We shall see the detailed numerical results in the following section.

4 Results

In this section we present the numerical computations of the velocity, the gravitational potential, and the lensing contributions to the correlation function of the luminosity distances. Especially, we discuss how the angular correlation function of the luminosity distances depends on the matter content today in a flat Λ CDM universe.

In principle, the integrations in the expression of the luminosity distance correlation function should be performed from zero-wavenumber to infinite-wavenumber i.e., $k_{\text{IR}} = 0$ and $k_{\text{UV}} = \infty$. However, as shown in [18], the contribution of super-horizon perturbation modes to the luminosity distance is negligible, if we use the gauge-invariant expression of the luminosity distance. Therefore, there is no significant numerical difference between the choices $k_{\text{IR}} = \mathcal{H}_o$ and $k_{\text{IR}} < \mathcal{H}_o$, and we set the lower cutoff as $k_{\text{IR}} = \mathcal{H}_o$. In the case of the upper cutoff choice, we set mostly $k_{\text{UV}} = 0.1 \text{ h/Mpc}$ since the nonlinearity becomes important at $k \gtrsim 0.1 \text{ h/Mpc}$. In fact, the larger k_{UV} yields the larger amplitude at a certain range $0.1 \text{ h/Mpc} \lesssim k_{\text{UV}} \lesssim 1 \text{ h/Mpc}$, and the upper cutoff choice does not yield significant difference at $k_{\text{UV}} \gtrsim 1 \text{ h/Mpc}$ (see [12]). We also discuss how numeric amplitudes depend on a choice of k_{UV} .

4.1 Angular correlation function of the luminosity distance ($z_1 = z_2$)

The angular correlation functions of the three contributions at $z = 0.5$ ($z = 1.0$) are illustrated in the upper left (right) figure in Fig. 3. The bottom panels show the fractional difference between the $\Omega_m = 0.3$ universe and others ($\Omega_m = 0.25$ and $\Omega_m = 0.35$). Note that the range of the angular separation is different in the left and the right panels since the coverage of a deep survey at high redshift is usually narrow.

The velocity contribution to the angular correlation function is important at redshift $z = 0.5$ for any angular separation, and at redshift $z = 1.0$ for $\theta \gtrsim 5^\circ$. The lensing contribution is dominant at $z = 1.0$ but only for small angular separation $\theta \lesssim 5^\circ$ since it decays sharply as the angular separation increases compared to the other contributions. As discussed in section 3, the gravitational potential contribution to the luminosity distance correlation function is nearly independent of the separation between sources, and its amplitudes are approximately $\mathcal{O}(10^{-8})$ at $z_1 = z_2 = 0.5$ and $\mathcal{O}(10^{-10})$ at $z_1 = z_2 = 1.0$. As a result, the gravitational potential contribution is always smaller than the other contributions, except for the lensing contribution at large separation. As shown in Fig. 3, the larger Ω_m yields the larger amplitude for the velocity contribution over the angular scales. However, the effect of Ω_m on the lensing

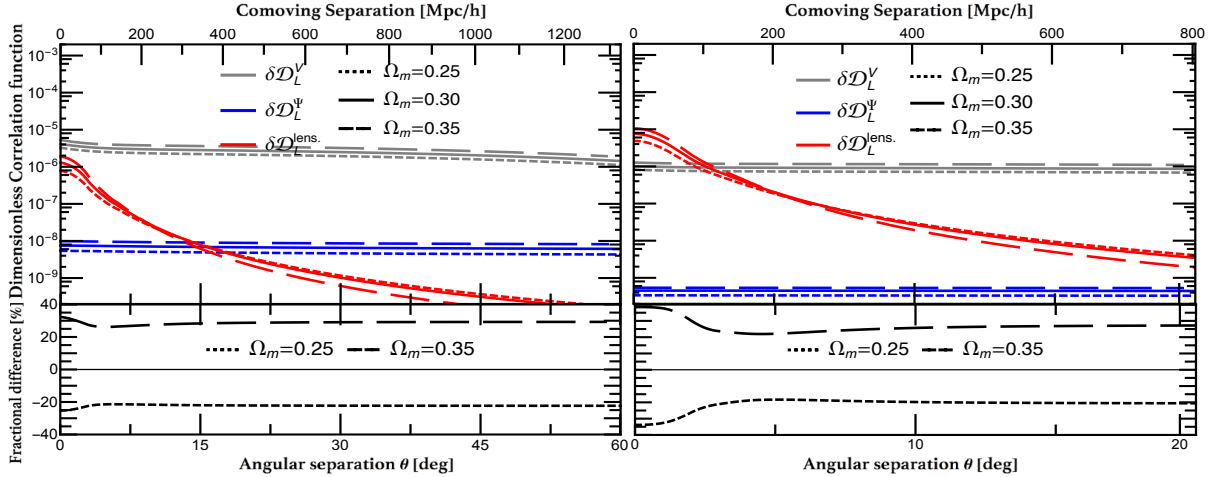


Figure 3: The left-top (right) figure shows the (dimensionless) angular correlation functions of $z = 0.5$ ($z = 1.0$), and the corresponding fractional differences between $\Omega_m = 0.3$ and others ($\Omega_m = 0.25$ and 0.35) are illustrated in the bottom figures. The grey, the blue, and the red lines indicate the velocity, the gravitational potential, and the lensing contributions, respectively. Different line types represent the different cosmological parameter sets: the dotted, the solid, and the dot-dashed lines corresponds to $\Omega_m = 0.25$, $\Omega_m = 0.3$, and $\Omega_m = 0.35$ in the flat Λ CDM universe, respectively. The conversion of the angle θ to the comoving separation is made by assuming $\Omega_m = 0.3$.

contribution is more complicated. Similarly to the velocity contribution, the lensing correlation function also increases as Ω_m increases but only for small angular separation, and this tendency becomes opposite when the angular separation is large. In the velocity contribution to the luminosity distance correlation function, the dominant contribution is the auto-correlation of the velocity at the observer's position (the third line in Eq. (3.3)), and it is proportional to $(\mathcal{C}D_{Vo})^2$, where $\mathcal{C}D_V = -\frac{d \ln D}{d \ln a} \mathcal{H}D$. In a Λ CDM universe, $\frac{d \ln D}{d \ln a}$ is simply expressed as $\frac{d \ln D}{d \ln a} \simeq \Omega_m^{0.55}$, and the $(\mathcal{C}D_{Vo})^2$ is proportional to $\Omega_m^{1.1}$. While the velocity contribution is proportional to $\Omega_m^{1.1}$, the lensing correlation is proportional to Ω_m^2 as presented in Eq. (3.4). As a result, the fractional difference between the universe with $\Omega_m = 0.3$ and the other cases ($\Omega_m = 0.25$ and $\Omega_m = 0.35$) is enhanced when the lensing contribution is significant (small angular separation and high redshift).

When we choose larger k_{UV} e.g., $k_{UV} = 10 h/\text{Mpc}$, the amplitude of the auto-correlation function of the contribution of the velocity at the observer increases with a factor of 1.5 as discussed previously in section 3, and this contribution is independent from the separations of sources. Thus, as k_{UV} increases from $k_{UV} = 0.1 h/\text{Mpc}$ to $k_{UV} = 1 h/\text{Mpc}$, the amplitude of $\langle \delta D_L^V \delta D_L^V \rangle$ increases at all separations until the angular separation reaches 90° . In addition, the lensing contribution is more sensitive on a larger k_{UV} choice, for instance, the maximum amplitude of $\langle \delta D_L^{\text{lens.}} \delta D_L^{\text{lens.}} \rangle$ with $k_{UV} = 1 h/\text{Mpc}$ ($k_{UV} = 10 h/\text{Mpc}$) is about 3.5 (5) times larger than that with $k_{UV} = 0.1 h/\text{Mpc}$ at $z = 0.5$ and $z = 1.0$. However, in contrast to the velocity contribution case, the amplitude of the lensing correlation increases just at small separations ($\theta \lesssim 3^\circ$) with respect to k_{UV} . At large separations, the change is insignificant, and the amplitude of the lensing contribution is also subdominant to the velocity contribution at any redshift.

4.2 Three-dimensional two-point correlation function of the luminosity distance ($z_1 \neq z_2$)

As discussed, the correlation functions of the velocity and the lensing contribution are anisotropic. For this reason, we present the correlation function as a function of the parallel and the perpendicular separations. These separations are defined in the midpoint coordinate illustrated in Fig. 4 (see also [29–31]). As depicted in Fig. 4, the midpoint vector \mathbf{r}_c points to the midpoint on the separation of the sources i.e., $\mathbf{r}_c = \frac{1}{2} (\bar{r}_{z_1} \hat{\mathbf{n}}_1 + \bar{r}_{z_2} \hat{\mathbf{n}}_2)$, where \bar{r}_{z_1} and \bar{r}_{z_2} are the comoving distances of the sources. Two distance

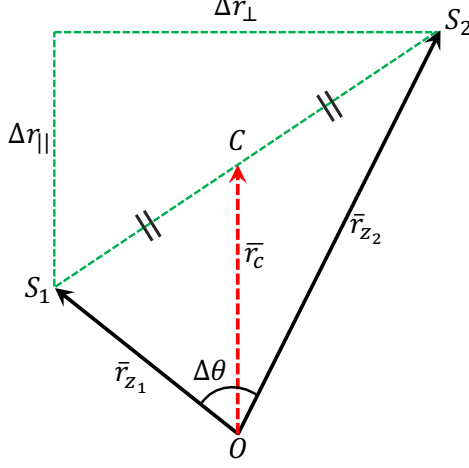


Figure 4: Points S_1 and S_2 denote the source positions whose vectors from the observation position O are \bar{r}_{z_1} and \bar{r}_{z_2} , respectively. $\Delta\theta$ is the angle between these two vectors. The point C is the midpoint which equally divides the connecting line between S_1 and S_2 , and the midpoint vector is \bar{r}_c . Δr_{\parallel} (Δr_{\perp}) indicates the parallel (perpendicular) separation with respect to the midpoint vector \bar{r}_c .

vectors can be expressed in terms of the parallel separation Δr_{\parallel} , the perpendicular separation Δr_{\perp} , and the midpoint distance from the observer \bar{r}_c by utilizing the Heron's formula and the geometric length of $\overline{OS_1}$ as³

$$\bar{r}_{z_1} = \frac{1}{2} \sqrt{(2\bar{r}_c - \Delta r_{\parallel})^2 + \Delta r_{\perp}^2}, \quad \bar{r}_{z_2} = \frac{1}{2} \sqrt{(2\bar{r}_c + \Delta r_{\parallel})^2 + \Delta r_{\perp}^2}, \quad (4.2)$$

The angular separation $\Delta\theta$ is determined from the geometric length between two sources as

$$\cos \Delta\theta = \frac{4\bar{r}_c^2 - \Delta r_{\parallel}^2 - \Delta r_{\perp}^2}{\bar{r}_{z_1} \bar{r}_{z_2}}. \quad (4.3)$$

For instance, $\hat{\mathcal{P}}_{\perp}$ and $\hat{\mathcal{P}}_{\parallel}$ in Eq. (3.3) are expressed in terms of \bar{r}_c , Δr_{\parallel} , and Δr_{\perp} as

$$\begin{aligned} \hat{\mathcal{P}}_{\parallel}(\bar{r}_z, \Delta r_{\parallel}, \Delta r_{\perp}) &= (\hat{n}_1 \cdot \hat{r})(\hat{n}_2 \cdot \hat{r}) = \frac{\bar{r}_{z_1} - \bar{r}_{z_2} \cos \Delta\theta}{\sqrt{\bar{r}_{z_1}^2 + \bar{r}_{z_2}^2 - 2\bar{r}_{z_1}\bar{r}_{z_2} \cos \Delta\theta}} \times \frac{\bar{r}_{z_1} \cos \Delta\theta - \bar{r}_{z_2}}{\sqrt{\bar{r}_{z_1}^2 + \bar{r}_{z_2}^2 - 2\bar{r}_{z_1}\bar{r}_{z_2} \cos \Delta\theta}} \\ &= -\frac{(\Delta r_{\parallel}^2 + \Delta r_{\perp}^2 - 2\bar{r}_c \Delta r_{\parallel})(\Delta r_{\parallel}^2 + \Delta r_{\perp}^2 + 2\bar{r}_c \Delta r_{\parallel})}{(\Delta r_{\parallel}^2 + \Delta r_{\perp}^2) \sqrt{\Delta r_{\perp}^2 + (\Delta r_{\parallel} - 2\bar{r}_c)^2} \sqrt{\Delta r_{\perp}^2 + (\Delta r_{\parallel} + 2\bar{r}_c)^2}}, \\ \hat{\mathcal{P}}_{\perp}(\bar{r}_z, \Delta r_{\parallel}, \Delta r_{\perp}) &= \hat{n}_1 \cdot \hat{n}_2 - \hat{\mathcal{P}}_{\parallel} = \cos \Delta\theta - \hat{\mathcal{P}}_{\parallel} \\ &= \frac{4\bar{r}_c^2 \Delta r_{\perp}^2}{(\Delta r_{\parallel}^2 + \Delta r_{\perp}^2) \sqrt{\Delta r_{\perp}^2 + (\Delta r_{\parallel} - 2\bar{r}_c)^2} \sqrt{\Delta r_{\perp}^2 + (\Delta r_{\parallel} + 2\bar{r}_c)^2}}. \end{aligned} \quad (4.4)$$

We numerically investigate the three-dimensional two-point correlation function of the luminosity distances for given midpoint distances: $\bar{r}_c \simeq 293 \text{ Mpc}/h$, $1323 \text{ Mpc}/h$, and $2314 \text{ Mpc}/h$, corresponding to redshifts $\bar{z}_c = 0.1$, $\bar{z}_c = 0.5$, and $\bar{z}_c = 1.0$ in a flat ΛCDM universe with $\Omega_m = 0.3$. The wide angle

³ The Heron's formula is

$$A = \sqrt{s(s-a)(s-b)(s-c)}, \quad (4.1)$$

where A is the area, a , b , and c are lengths of each side. s is defined as $s \equiv \frac{a+b+c}{2}$.

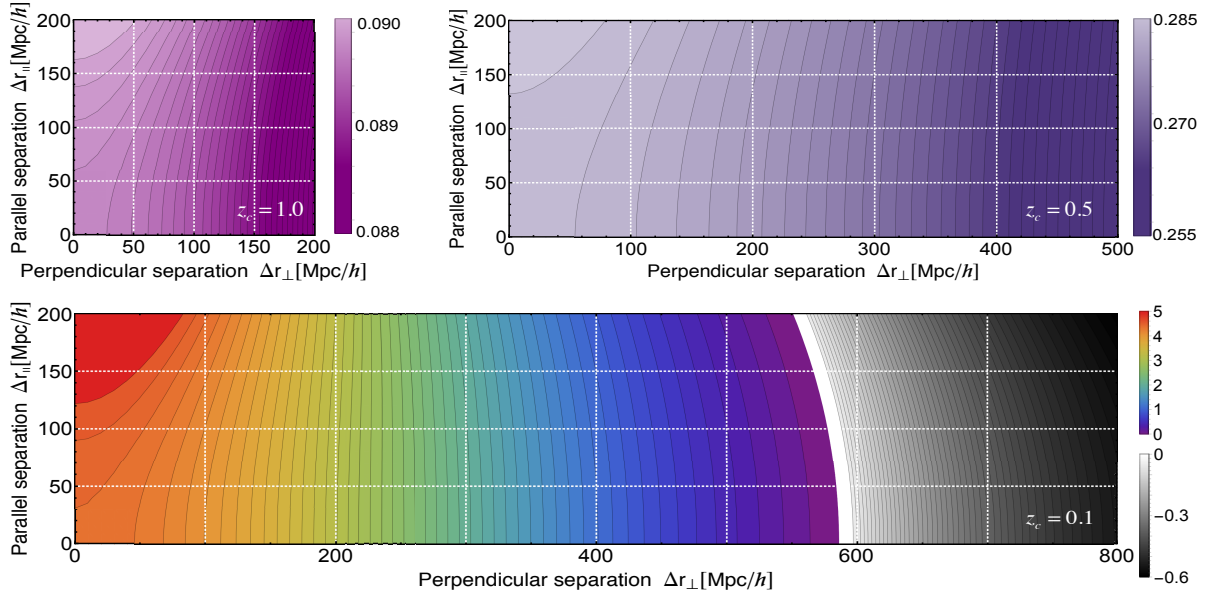


Figure 5: Auto-correlation of the observer velocity contribution of the flat Λ CDM universe of $\Omega_m = 0.3$. The amplitudes are multiplied by 10^5 e.g., 5 in the figure means 5×10^{-5} . The rainbow (gray) color indicates the positive (negative) correlation. The navy ($\bar{z}_c = 0.5$) and the purple ($\bar{z}_c = 1.0$) unicolors with gradations describe subtle changes of their amplitude with respect to Δr_{\parallel} and Δr_{\perp} . The result with the midpoint redshift $\bar{z}_c = 0.1$ is shown in the bottom, and that with $\bar{z}_c = 0.5$ is presented in the right upper figure. The left top figure corresponds to that with $\bar{z}_c = 1.0$.

effect, which originates from the difference in the two line-of-sights of sources, is taken into account in the results. The predicted noise σ_{mm} on the correlation is presented in [23] as

$$\sigma_{\text{mm}} = \frac{\sigma_{\text{err}}^2}{\sqrt{N_p}}, \quad (4.5)$$

where σ_{err} is the overall uncertainty on individual supernova magnitude measurements, and N_p is the number of pairs within a certain angular separation $[\theta, \theta + \delta\theta]$. The explicit expression of N_p is $N_p = N_s(N_s - 1)\pi\theta\Delta\theta/A_{\text{survey}}$, where N_s is the number of source which is uniformly distributed on the survey area A_{survey} . With σ_{mm} , the signal-to-noise (SNR) of the correlation function of the luminosity distances becomes

$$\text{SNR} = \frac{\langle \delta\mathcal{D}_L(z_1, \hat{n}_1)\delta\mathcal{D}_L(z_2, \hat{n}_2) \rangle}{\sigma_{\text{mm}}}. \quad (4.6)$$

In the case of the deep LSST survey, the number of source and the survey area are $N_s \simeq 10^4$, $A_{\text{survey}} = 20 \text{ deg}^2$, and the overall uncertainty in current observation is $\sigma_{\text{err}} \simeq 0.1$. Thus, the predicted noise in this case is $\sigma_{\text{mm}} \sim 10^{-5}$ when the angular separation and the angular bin size are approximately $\theta = 5^\circ$ and $\delta\theta = 0.01^\circ$, respectively. To compare the amplitudes of the correlation function and of the estimated noise, the amplitudes of figures are multiplied by 10^5 .

Figures 5, 6, and 7 show the results of the velocity at the observation, the source velocity, the lensing contributions. The sum of all the correlation functions with different midpoint redshifts are illustrated in Fig. 8. The white line indicates the contour, at which correlation vanishes. The gray color is used to represent negative values i.e., anti-correlated region. When the magnitude in a figure changes dramatically, we make the figure with the rainbow color. In the opposite case, we use unicolor to depict subtle changes. Each figure consists of three sub-figures, and the midpoint redshifts of the sub-figures are different. Among these sub-figures, the ranges of the parallel separation are same but that of the

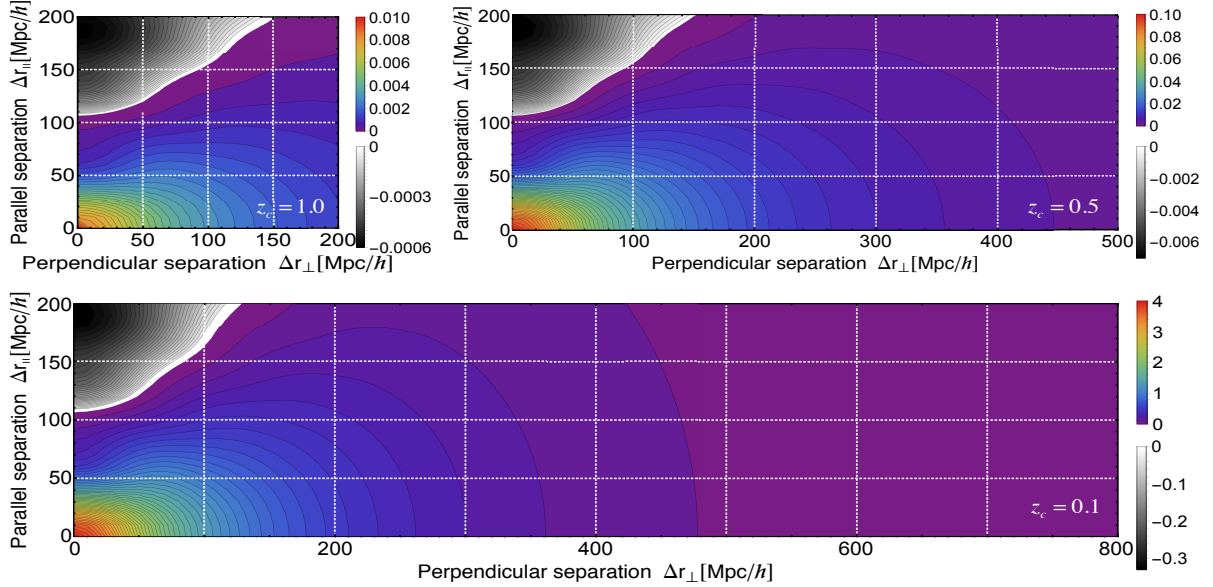


Figure 6: Auto-correlation of the source velocity contribution in the same format as Fig. 5.

perpendicular separations are different. The reason is that the angular coverage is usually large for small redshift surveys.

The correlation function of the observer velocity contribution is depicted in Fig. 5. As discussed in Eq. (3.3), the correlation of the observer velocity contribution vanishes when the angular separation between sources $\Delta\theta$ is $\Delta\theta = 90^\circ$, and it becomes anti-correlated beyond this angular separation. Since the auto-correlation function of the observer velocity does not depend on the comoving separation between sources, the position dependency of the observer velocity contribution only comes from the coefficient of the observer velocity $(\mathcal{H}_z \bar{r}_z)^{-1}$ in Eq. (2.2). In other words, the observer velocity contribution has the larger signal as the source is closer regardless of the separation between sources. As a result, the largest signal in Fig. 5 manifests at $(\Delta r_\perp, \Delta r_\parallel) = (0, 200)$ where $(\bar{r}_{z_1}, \bar{r}_{z_2}) = (193, 393), (1223, 1423), (2214, 2414)$ for $\bar{z}_c = 0.1, 0.5, 1.0$. The auto-correlation becomes smaller in general as the redshift of midpoint increases. For redshift $\bar{z}_c = 0.5$ and $\bar{z}_c = 1.0$, the sources' comoving distances from the observer are much larger than the parallel and the perpendicular separations. Thus, the amplitude changes very little with respect to the separations. For this reason, the plots of the observer velocity auto-correlation function of $\bar{z}_c = 0.5$ and $\bar{z}_c = 1.0$ are made with unicolors.

As discussed in Eq. (3.3) and also in Fig. 1, the auto-correlation function of the source velocity contribution in Fig. 6 depends not only on the distance between source and observer but also on the separation between sources. The strong signal appears at small separation where ξ_\parallel and ξ_\perp are largest. In addition, the auto-correlation function of the source velocity contribution naturally becomes negative when $\Delta r_\parallel > 100 \text{ Mpc}/h$ and the parallel component is larger than the perpendicular component. For large perpendicular separation ($\Delta r_\perp \gtrsim 500 \text{ Mpc}/h$), the signal is almost constant because of the decay of ξ_\perp in Fig. 1.

The auto-correlation of the lensing contribution is presented in Fig. 7. As investigated in the angular correlation function, it sharply decays as the perpendicular distance (or the angle) increases in the vicinity of the zero separation, and it becomes almost constant when $\Delta r_\perp \gtrsim 100 \text{ Mpc}/h$. By contrast, the dependency on parallel separation is very weak because the lensing contribution arises from the fluctuations projected along the line-of-sight ($\Delta r_\parallel \ll \bar{r}_c$). However, it can weakly depend on

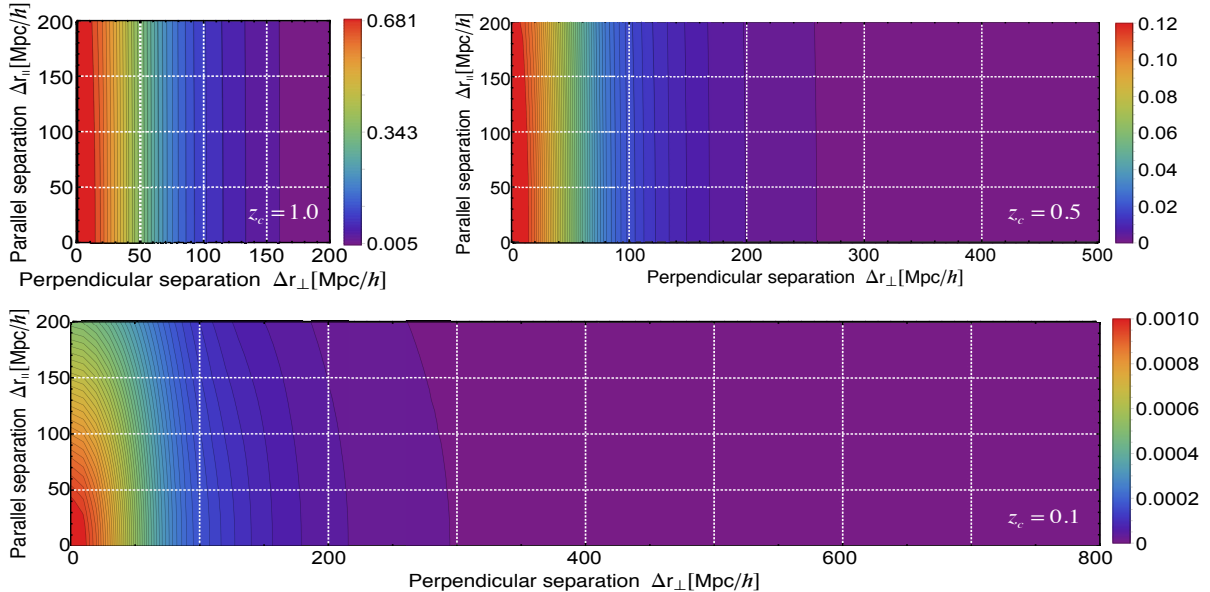


Figure 7: Auto-correlation of the lensing contribution in the same format as Fig. 5.

Δr_{\parallel} at low redshift, where $\Delta r_{\parallel} \simeq \bar{r}_c$.

We illustrate the total correlation function of all the contributions in Fig. 8. Analogous to the angular correlation function in Fig. 3, the velocity contribution dominates for the small midpoint redshift ($\bar{z}_c = 0.1$). In this case, the anti-correlated region of the source velocity contribution is compensated by the large amplitude of the observer velocity contribution, and this region becomes positively correlated in the total one. When the angular separation is larger than 90° , the auto-correlation of the observer velocity contribution becomes anti-correlated, and its amplitude is larger than the other contributions. As a result, the sum of all the correlations becomes anti-correlated for $\Delta\theta > 90^\circ$. In contrast to the result of small midpoint redshift, the total correlation function of the luminosity distance at $\bar{z}_c = 1.0$ is strongly influenced by the lensing contribution. In this case, the source velocity contribution is fully suppressed by the others. The auto-correlation of the observer velocity contribution is almost constant and it is larger than the lensing contribution for sufficiently large perpendicular separation ($\Delta r_{\perp} \gtrsim 80$ Mpc/h). As a result, the total correlation at the small perpendicular separation is governed by the lensing contribution and that at the large perpendicular separation is almost constant. The case of the midpoint redshift $\bar{z}_c = 0.5$ is more interesting since the three contributions are all equally important, but its largest signal is still smaller than those in the other cases. For the case of small Δr_{\perp} , the elongation along Δr_{\parallel} manifests due to the lensing contribution.

5 Discussion

In this paper we have computed the two-point correlation function of the luminosity distances. We decomposed the luminosity distance fluctuation into the velocity, the gravitational potential, and the lensing contributions, and we have numerically evaluated each contribution. Especially, we presented the velocity at the observer position and gravitational potential contributions to the luminosity distance correlation function for the first time.⁴ The features of each contribution are as follows. The lensing

⁴Here we do not consider the observed peculiar velocity with respect to the CMB rest frame, in which the observed CMB dipole vanishes.

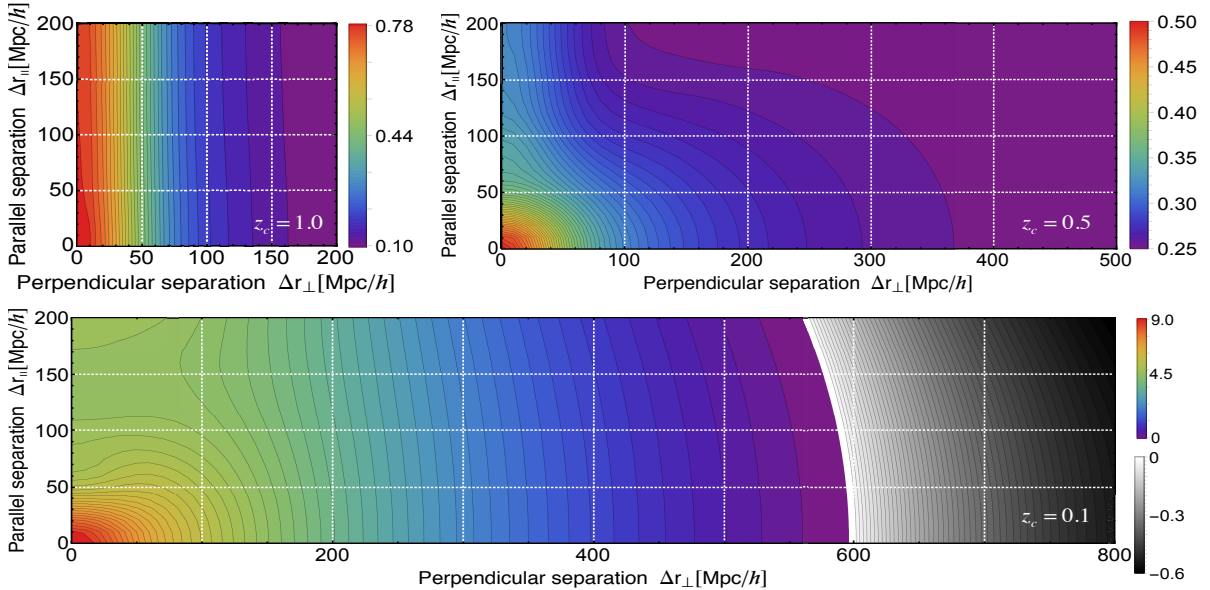


Figure 8: Correlation function of the luminosity distance in the same format as Fig. 5. The (total) correlation function is the sum of all auto-correlations in Figures 5 to 7 and their cross-correlations.

contribution dominates over the other contributions at angular separations ($\theta \lesssim 5^\circ$) and large redshift ($z \gtrsim 0.5$), while the velocity contribution is the key contribution in all the other cases where the lensing contribution is small. In contrast, the gravitational potential contribution is always subdominant to the sum of the other correlation functions, if the proper gauge-invariant expression is used. We also investigated the dependence of the correlation function of the luminosity distances on the current matter content Ω_m , and as Ω_m increases, the amplitude grows substantially. For instance, the fractional difference between the $\Omega_m = 0.3$ and the $\Omega_m = 0.25$ (or $\Omega_m = 0.35$) amplitudes is about 30% – 40% at $z = 0.5$ and $z = 1.0$. Especially, not only the amplitude but also the shape of the lensing correlation is affected strongly by Ω_m value.

The expressions of the velocity and the lensing contributions to the luminosity distance are in agreement with the previous studies (e.g. [10, 11, 21]). From these expressions, one can derive the correlation functions of each expression. The contributions of the velocity at the source position and of the lensing to the correlation function of the luminosity distance are presented respectively in [32] and [23], and they correspond to the results in this paper. However, the expression of the gravitational potential contribution to the luminosity distance in this paper is in disagreement with the previous research, except for [6–9], due to the absence of the coordinate lapse at the observation.

As shown in [18], the gravitational potential contribution without the coordinate lapse at the observation breaks the gauge-invariance of the luminosity distance, and this absence leads to the infrared divergence in the computation of the luminosity distance correlation function. That is, the gravitational potential contribution becomes the most dominant one when perturbations on sufficiently large scales ($k_{\text{IR}} \rightarrow 0$) are included. However, these two problems (violation of the gauge-invariance and the manifestation of the infrared divergence) are resolved altogether by taking into account the coordinate lapse at the observation and by using the full gauge-invariant expression for the luminosity distance. With such proper expression, we showed that the gravitational potential contribution to the correlation function of the luminosity distance is completely negligible, even if we choose very small k_{IR} . However, the contribution of the gravitational potential without the coordinate lapse at the observer position is very close to that of the gravitational potential with the coordinate lapse when we consider only sub-horizon

perturbation modes since the contribution of the coordinate lapse at the observation is only sensitive on super-horizon perturbation modes.

In observation, the observed redshift is corrected by accounting for the peculiar motion ($v_{\text{dip}} \simeq 371$ km/s [25]) of the observer, which is defined as the velocity needed to transform to the CMB rest frame. Since this observed peculiar velocity is well defined and independent of our gauge choice, this observational procedure of correcting the redshift causes no theoretical problems. However, providing a theoretical description of such procedure requires a gauge-invariant expression of the observed peculiar velocity with respect to the CMB rest frame, which is beyond our current scope. In contrast, one cannot simply remove the velocity contribution at the observer position in any chosen gauge condition, in order to match the observational procedure, as was done in previous work (e.g. [15, 21, 22]). For instance, the peculiar velocity field is absent in the synchronous gauge, but the luminosity distance in the synchronous gauge is equivalent to that in the other gauges due to the gauge-invariance of the luminosity distance. Therefore, if one removes the observer velocity in the conformal Newtonian gauge, it is already apparent that the resulting outcome is gauge-dependent. Second, as shown in [18], the luminosity distance without the velocity at the observation position violates the equivalence principle, although it should be fully respected in general relativity. Furthermore, neglecting such contribution yields substantial numerical errors.

The signal-to-noise ratio of the lensing contribution to the correlation function of type Ia supernovae is investigated in [23]. According to this study, the lensing contribution to the correlation function of the luminosity distances is detectable for the deep LSST survey, where the supernova number distribution has a peak around $z \simeq 0.5$ and the coverage is 70 deg^2 . As discussed in this paper, the velocity contribution is also comparable to the lensing contribution when sources' redshifts are around $z \sim 0.5$, and the signal-to-noise should be enhanced, taking into account the velocity contribution. That is, the correlation function of the luminosity distances is expected to be observed in the deep LSST survey, and it can be utilized as a novel tool of estimating cosmological parameters.

The dispersion of the luminosity distance measurement originates not only from the intrinsic scatter of supernovae but also from the luminosity distance fluctuation due to the inhomogeneity of the universe. In contrast to the intrinsic scatter, the fluctuation due to the inhomogeneity yields systematic errors to the Hubble diagram. As a result, the mean luminosity distance in an inhomogeneous universe $\langle \mathcal{D}_L \rangle$ might somewhat differ from the luminosity distance in a homogeneous universe $\bar{\mathcal{D}}_L$. To study this, we need to derive the second-order expression for the luminosity distance, beyond the scope of this paper, and the z_{dip} effect might play an important role at this level. In fact, this computation was already performed in a few studies [14, 27]. However, it has never been shown that the second order expressions are gauge-invariant and consistent with the equivalence principle (or at least consistent with each other). It is noted [18] that previous studies at the linear order often do not satisfy these requirements (gauge-invariance and consistency with the equivalence principle). A proper gauge-invariant calculation at the second order will be needed to completely settle the issue and quantify the shift in the mean of the luminosity distance.

Acknowledgments

We acknowledge support by the Swiss National Science Foundation, and J.Y. is further supported by a Consolidator Grant of the European Research Council (ERC-2015-CoG grant 680886).

A The auto-correlation function of the gravitational potential contribution

The correlation function of the gravitational potential contribution can be decomposed into auto- and cross-correlations as $\langle \delta \mathcal{D}_L^\Psi(z_1, \hat{\mathbf{n}}_1) \delta \mathcal{D}_L^\Psi(z_2, \hat{\mathbf{n}}_2) \rangle = \xi_{ss}^\Psi + \xi_{so}^\Psi + \xi_{oo}^\Psi + \xi_{si}^\Psi + \xi_{oi}^\Psi + \xi_{ii}^\Psi$, representing the

contributions at the source (s) and the observer (o), and the line-of-sight contributions (i). The detailed expressions of each term are

$$\begin{aligned}
\xi_{ss}^{\Psi} &= h_1(z_1)h_1(z_2)D_{\Psi_1}D_{\Psi_2}\xi_{\zeta}(|\mathbf{r}|), \tag{A.1} \\
\xi_{oo}^{\Psi} &= \left\{ \left(\frac{1}{\bar{r}_{z_1}} - \mathcal{H}_o h_1(z_1) \right) D_{V_o} - h_2(z_1)D_{\Psi_o} \right\} \times (1 \leftrightarrow 2) \xi_{\zeta}(0), \\
\xi_{ii}^{\Psi} &= 4\mathcal{H}_{z_1}\mathcal{H}_{z_2}h_2(z_1)h_2(z_2) \int_0^{\bar{r}_{z_1}} d\bar{r}_1 \int_0^{\bar{r}_{z_2}} d\bar{r}_2 \{ D_{\Psi}(\bar{\tau}_o - \bar{r}_1)D_{\Psi}(\bar{\tau}_o - \bar{r}_2) + f_1(\Psi', \Psi'') \} \xi_{\zeta}(|\bar{r}_1\hat{n}_1 - \bar{r}_2\hat{n}_2|), \\
\xi_{so}^{\Psi} &= \left\{ \left(\frac{1}{\bar{r}_{z_1}} - \mathcal{H}_o h_1(z_1) \right) D_{V_o} - h_2(z_1)D_{\Psi_o} \right\} h_1(z_2)D_{\Psi_2}\xi_{\zeta}(\bar{r}_{z_2}) + (1 \leftrightarrow 2), \\
\xi_{oi}^{\Psi} &= 2\mathcal{H}_{z_2}h_2(z_2) \left\{ \left(\frac{1}{\bar{r}_{z_1}} - \mathcal{H}_o h_1(z_1) \right) D_{V_o} - h_2(z_1)D_{\Psi_o} \right\} \int_0^{\bar{r}_{z_2}} d\bar{r}_2 \{ D_{\Psi}(\bar{\tau}_o - \bar{r}_2) + f_2(\Psi', \Psi'') \} \xi_{\zeta}(\bar{r}_2) \\
&\quad + (1 \leftrightarrow 2), \\
\xi_{si}^{\Psi} &= 2\mathcal{H}_{z_2}h_1(z_1)h_2(z_2)D_{\Psi_1} \int_0^{\bar{r}_{z_2}} d\bar{r}_2 \{ D_{\Psi}(\bar{\tau}_o - \bar{r}_2) + f_2(\Psi', \Psi'') \} \xi_{\zeta}(|\bar{r}_{z_1}\hat{n}_1 - \bar{r}_2\hat{n}_2|) + (1 \leftrightarrow 2),
\end{aligned}$$

where $h_1(z_i)$ and $h_2(z_i)$ are defined as $h_1(z_i) \equiv \left(\frac{1}{\mathcal{H}_{z_i}\bar{r}_{z_i}} - 1 \right)$ and $h_2(z_i) \equiv \frac{1}{\mathcal{H}_{z_i}\bar{r}_{z_i}}$, $f_1(\Psi', \Psi'')$ and $f_2(\Psi', \Psi'')$ indicate the (negligible) contributions of Ψ' and Ψ'' in Eq. (2.2), and ξ_{XX}^{Ψ} and ξ_{XY}^{Ψ} represent respectively the auto- and the cross-correlation functions ($X, Y = s, o, i$).

References

- [1] S. Perlmutter et al., *Astrophys. J.* **517**, 565 (1999), [arXiv:astro-ph/9812133](#).
- [2] A. G. Riess et al., *Astron. J.* **116**, 1009 (1998), [arXiv:astro-ph/9805201](#).
- [3] P. A. R. Ade et al., *Astron. Astrophys.* **571**, A16 (2014), [arXiv:1303.5076](#).
- [4] D. J. Eisenstein, I. Zehavi, D. W. Hogg, R. Scoccimarro, et al., *Astrophys. J.* **633**, 560 (2005), [astro-ph/0501171](#).
- [5] P. A. Abell et al. (LSST), [arXiv:0912.0201](#).
- [6] M. Sasaki, *Mon. Not. R. Astron. Soc.* **228**, 653 (1987).
- [7] J. Yoo, *Class. Quant. Grav.* **31**, 234001 (2014), [arXiv:1409.3223](#).
- [8] D. Jeong, F. Schmidt, and C. M. Hirata, *Phys. Rev. D* **85**, 023504 (2012), [arXiv:1107.5427](#).
- [9] F. Schmidt and D. Jeong, *Phys. Rev. D* **86**, 083527 (2012), [arXiv:1204.3625](#).
- [10] C. Bonvin, R. Durrer, and M. A. Gasparini, *Phys. Rev. D* **73**, 023523 (2006), [arXiv:0511183](#).
- [11] D. J. Bacon, S. Andrianomena, C. Clarkson, K. Bolejko, and R. Maartens, *Mon. Not. R. Astron. Soc.* **443**, 1900 (2014), [arXiv:1401.3694](#).
- [12] I. Ben-Dayan, M. Gasperini, G. Marozzi, F. Nugier, and G. Veneziano, *J. Cosmol. Astropart. Phys.* **4**, 036 (2012), [arXiv:1202.1247](#).
- [13] I. Ben-Dayan, G. Marozzi, F. Nugier, and G. Veneziano, *J. Cosmol. Astropart. Phys.* **11**, 045 (2012), [arXiv:1209.4326](#).
- [14] I. Ben-Dayan, M. Gasperini, G. Marozzi, F. Nugier, and G. Veneziano, *J. Cosmol. Astropart. Phys.* **6**, 002 (2013), [arXiv:1302.0740](#).
- [15] I. Ben-Dayan, R. Durrer, G. Marozzi, and D. J. Schwarz, *Physical Review Letters* **112**, 221301 (2014), [arXiv:1401.7973](#).

- [16] G. Fanizza, M. Gasperini, G. Marozzi, and G. Veneziano, *J. Cosmol. Astropart. Phys.* **11**, 019 (2013), [arXiv:1308.4935](#).
- [17] M. Gasperini, G. Marozzi, F. Nugier, and G. Veneziano, *J. Cosmol. Astropart. Phys.* **7**, 008 (2011), [arXiv:1104.1167](#).
- [18] S. G. Biern and J. Yoo, *J. Cosmol. Astropart. Phys.* **1704**, 045 (2017), [arXiv:1606.01910](#).
- [19] J. Yoo and J. O. Gong, *J. Cosmol. Astropart. Phys.* **7**, 017 (2016), [arXiv:1602.06300](#).
- [20] J. Yoo and F. Scaccabarozzi, *J. Cosmol. Astropart. Phys.* **1609**, 046 (2016), [arXiv:1606.08453](#).
- [21] L. Hui and P. B. Greene, *Phys. Rev. D* **73**, 123526 (2006), [astro-ph/0512159](#).
- [22] D. L. Huterer, D. Shafer and F. Schmidt, *J. Cosmol. Astropart. Phys.* **12**, 033 (2015), [arXiv:1509.04708](#).
- [23] D. Scovacricchi, R. C. Nichol, E. Macaulay, and D. Bacon, [arXiv:1611.01315](#).
- [24] A. Cooray, D. E. Holz, and D. Huterer, *Astrophys. J.* **637**, L77 (2006), [astro-ph/0509579](#).
- [25] N. Aghanim et al. (Planck), *Astron. Astrophys.* **571**, A27 (2014), [arXiv:1303.5087](#).
- [26] N. Kaiser, and J. Hudson, *Mon. Not. R. Astron. Soc.* **450**, 883-895, (2014), [arXiv:1411.6339](#).
- [27] E. Barausse, S. Matarrese, and A. Riotto, *Phys. Rev. D* **71**, 063537 (2005), [astro-ph/0501152](#).
- [28] P. Simon, *Astron. Astrophys.* **473**, 711, (2007), [astro-ph/0609165](#).
- [29] K. Yamamoto, M. Nakamichi, M. Kamino, B. A. Bassett, and H. Nishioka, *PASJ*, **58**, 93, (2006), [astro-ph/0505115](#).
- [30] L. Samushia, E. Branchini, and W. J. Percival, *Mon. Not. R. Astron. Soc.*, **452**, 4, (2015), [arXiv:1504.02135](#).
- [31] D. Bianchi, H. Gil-Marín, R. Ruggeri, and W. J. Percival, *Mon. Not. R. Astron. Soc.*, **453**, 1, (2015), [arXiv:1505.05341](#).
- [32] T. M. Davis et al., *Astrophys. J.* **741**, 67 (2011), [arXiv:1012.2912](#).
- [33] E. Macaulay et al., [arXiv:1607.03966](#).
- [34] I. Ben-Dayan, and R. Takahashi, *Mon. Not. R. Astron. Soc.*, **455**, 552, (2016), [arXiv:1504.07273](#).
- [35] I. Ben-Dayan, and T. Kalaydzhyan, *Phys. Rev. D*, **90**, 083509, (2014), [arXiv:1309.4771](#)
- [36] I. Ben-Dayan, [arXiv:1408.3004](#) [astro-ph.CO].